Synthesis, Structure, and Characterization of Five-Coordinate Aquo(octaethylporphinato)iron(III) Perchlorate

Beisong Cheng,[1a] Martin K. Safo,[1a] Robert D. Orosz,[1b] Christopher A. Reed,*[,1b] Peter G. Debrunner,*[,1c] and W. Robert Scheidt*[,1a]

Department of Chemistry and Biochemistry, University of Notre Dame, Notre Dame, Indiana 46556, Department of Chemistry, University of Southern California, Los Angeles, California 90089-0744, and Department of Physics, University of Illinois, Urbana, Illinois 61801

Received July 28, 1993®

Acid treatment of the μ-oxo bridge in (μ-oxo)(octaethylporphinato)iron(III) leads to $[Fe(OEP)(H_2O)]ClO_4$ or $\{[Fe(OEP)]_2(OH)\}ClO_4$ rather than the expected perchlorato or bis(aquo) species. Synthetic procedures, the X-ray structure determination, and Mössbauer and magnetic susceptibility measurements for aquo(octaethylporphinato)-iron(III) perchlorate, $[Fe(OEP)(H_2O)]ClO_4\cdot 2H_2O$ are described. The Mössbauer spectrum (at 4.2 K) shows a quadrupole doublet with a large splitting of ΔE_q = 3.287(5) mm/s and an isomer shift of 0.391(5) mm/s. The temperature-dependent magnetic susceptibility data are understood in terms of an admixed intermediate-spin state ($S = {}^3/_2, {}^5/_2$) and are readily fit to a Maltempo model with two interacting iron(III) centers and parameters $g_\perp$ = 4.65, ζ = 150 cm^{-1}, and J = −1.0 cm^{-1}. This dimeric model is consistent with the low-temperature (T = 124 K) crystal structure which reveals $[Fe(OEP)(H_2O)]_2^{2+}$ units. These are formed by a π–π interaction between cations with an Fe···Fe distance of 5.08 Å, a lateral shift of 3.39 Å, and an interplanar spacing of 3.39 Å between the mean planes of the cores. These dimeric units are further linked together into an infinite linear chain by a hydrogen bond network involving the axial aquo ligands, the perchlorate anions, and two additional water molecules per iron porphyrin unit. In the $[Fe(OEP)(H_2O)]^+$ cation, the average Fe–N_p distance is 1.982(4) Å, the axial Fe–O distance is 2.045(3) Å, and the iron atom is displaced 0.20 Å from the 24-atom mean plane. These structural data are consistent with an admixed intermediate-spin state for iron(III). Crystal data for $[Fe(OEP)(H_2O)]ClO_4\cdot 2H_2O$: $T = 124 \pm 2$ K, a = 12.169(1) Å, b = 13.388(11) Å, c = 13.409(10) Å, α = 62.71(6)°, β = 88.65(6)°, γ = 67.97(6)°, V = 1770.2(2.5) Å^3, triclinic, space group $P\bar{1}$, Z = 2, R_1 = 0.046, and R_2 = 0.064 for 4817 observed data. In attempted syntheses of a diaquo complex, we have isolated and structurally characterized the known compound $[Fe(OEP)(THF)_2]ClO_4$; more precise structural results are reported. Crystal data for $[Fe(OEP)(THF)_2]ClO_4$: $T = 292 \pm 1$ K, a = 13.918(1) Å, b = 16.519(6) Å, c = 10.654(2) Å, β = 118.21(2)°, V = 2158.5(5.3) Å^3, monoclinic, space group $C2/m$, Z = 2, R_1 = 0.054, and R_2 = 0.059 for 2263 observed data.

Introduction

It has long been recognized that treatment of μ-oxo-bridged iron(III) porphyrinates with acids leads to bridge cleavage and formation of monomeric species. Thus, for example, Straub[2] reported the preparation and characterization of a series of [Fe(TPP)X][3] derivatives prepared by HX cleavage of $[Fe(TPP)]_2O$. Dolphin et al.[4] also reported that $Fe(OEP)ClO_4$ and "$Fe(OEP)ClO_4\cdot 2EtOH$" were formed by breaking the μ-oxo bridge of $[Fe(OEP)]_2O$ with aqueous perchloric acid followed by treatment with EtOH. Recently, we communicated[5] that a novel hydroxo-bridged iron(III) porphyrinate, $\{[Fe(OEP)]_2(OH)\}^+$, could be formed by apparent protonation of the μ-oxo bridge when only a limited amount of acid was used in the reaction. In this μ-oxo bridge protonation reaction, less than 1 equiv of protons must be used. At even slightly higher proton concentrations, a new iron(III) complex began to be formed. An X-ray structure determination confirmed its formulation as $[Fe(OEP)(H_2O)]ClO_4$. Further studies on the synthesis of this monoaquo species showed that when reaction conditions (acid concentration) similar to that of Dolphin et al. were applied, this compound is the only product formed. Herein, we report the synthesis, crystal and molecular structure, and spectroscopic and magnetic characterization of $[Fe(OEP)(H_2O)]ClO_4\cdot 2H_2O$. We have also investigated whether a diaquo complex $[Fe(OEP)(H_2O)_2]ClO_4$, analogous to the known $[Fe(TPP)(H_2O)_2]ClO_4$,[6] could be isolated.

Experimental Section

General Information. H_2OEP was purchased from Midcentury Chemicals, $AgClO_4$ and $HClO_4$ were purchased from Aldrich, and all other reagents were obtained from Fisher. All materials were used as received; $FeCl_2$ was dried under vacuum (~250 °C) before use. $[Fe(TPP)]_2O$ and $[Fe(OEP)]_2O$ were prepared by following literature methods.[7] IR spectra were recorded on a Perkin-Elmer 883 infrared spectrophotometer as KBr pellets; electronic spectra were recorded on a Perkin-Elmer Lambda 19 UV/vis/near-IR spectrometer. EPR spectra were collected at 77 K on a Varian E-line spectrometer operating at X-band frequency. Mössbauer spectra were measured on ground crystals as Apiezon grease suspensions at 4.2 and 200 K. Magnetic susceptibility measurements at 2 and 10 kG were obtained on crushed crystals over the temperature range 6–280 K on a SHE 905 SQUID susceptometer.

Synthesis of $[Fe(OEP)(H_2O)]ClO_4\cdot 2H_2O$. Method 1. $[Fe(OEP)]_2O$ (69 mg, 0.057 mmol) in 10 mL of CH_2Cl_2 was reacted with 15 mL of

* Abstract published in *Advance ACS Abstracts*, March 1, 1994.

(1) (a) University at Notre Dame. (b) University of Southern California. (c) University of Illinois at Urbana-Champaign.

(2) Maricondi, C.; Swift, W.; Straub, D. K. *J. Am. Chem. Soc.* **1969**, *91*, 5205.

(3) Abbreviations used in this paper: OEP, the dianion of octaethylporphyrin; TPP, the dianion of 5,10,15,20-tetraphenylporphyrin; EtOH, ethanol; THF, tetrahydrofuran; X, halide or pseudohalide; N_p, porphinato nitrogen atom; Ct, center of the porphyrin ring.

(4) Dolphin, D. H.; Sams, J. R.; Tsin, T. B. *Inorg. Chem.* **1977**, *16*, 711.

(5) Scheidt, W. R.; Cheng, B.; Safo, M. K.; Cukiernik, F.; Marchon, J.-C.; Debrunner, P. G. *J. Am. Chem. Soc.* **1992**, *114*, 4420.

(6) Scheidt, W. R.; Cohen, I. A.; Kastner, M. E. *Biochemistry* **1979**, *18*, 3546.

(7) (a) Sadasivan, N.; Eberspaecher, H. I.; Fuchsman, W. H.; Caughey, W. S. *Biochemistry* **1969**, *8*, 534. (b) La Mar, G. N.; Eaton, G. R.; Holm, R. H.; Walker, F. A. *J. Am. Chem. Soc.* **1973**, *95*, 63. (c) O'Keeffe, D. H.; Barlow, C. H.; Smythe, G. A.; Fuchsman, W. H.; Moss, T. H.; Lilienthal, H. R.; Caughey, W. S. *Bioinorg. Chem.* **1975**, 125. (d) Hoffman, A. B.; Collins, D. M.; Day, V. W.; Fleischer, E. B.; Srivastava, T. S.; Hoard, J. L. *J. Am. Chem. Soc.* **1972**, *94*, 3620–3626.

0020-1669/94/1333-1319$04.50/0

aqueous $HClO_4$ (1.11×10^{-2} M, 0.167 mmol). The mixed-phase solution was stirred for 10 min, the water layer was separated, and the CH_2Cl_2 solution was dried with solid Na_2SO_4. The filtrate was taken to dryness, redissolved in 5 mL of CH_2Cl_2, and crystallized by diffusion of hexane. After several days, crystalline materials were collected, and microscopic examination suggested two products. The products were shown to be $[Fe(OEP)(H_2O)]ClO_4 \cdot 2H_2O$ (black platelike crystals) and the previously reported[5] $\{[Fe(OEP)]_2(OH)\}ClO_4$ (crystals decay very quickly) by X-ray analysis. *Caution!* Although we have experienced no problem with the procedures described in this work in dealing with systems containing perchlorate ion, they can detonate spontaneously and should be handled only in small quantities; in no case should such a system be heated above 30 °C, and other safety precautions are also warranted.

Method 2. A CH_2Cl_2 solution of $[Fe(OEP)]_2O$ (~50 mL, ~500 mg) was reacted with 100 mL of aqueous $HClO_4$ (~3 M). The aqueous phase was discarded, and the CH_2Cl_2 phase was washed with 100 mL of water. The CH_2Cl_2 phase was separated, dried with solid Na_2SO_4, and filtered. The UV–vis spectrum of this filtrate was essentially identical to that of single crystals of $[Fe(OEP)(H_2O)]ClO_4$ from method 1. Crystals of $[Fe(OEP)(H_2O)]ClO_4$ could be reproducibly obtained by crystallization of the filtrate. IR (ν_{ClO_4}): 1121 (s), 1108 (s), 1090 (s), 626 (m) cm^{-1}. UV–vis–near-IR (CH_2Cl_2): λ_{max} (ϵ, cm^{-1} M^{-1}) 386 (1.07×10^5), 500 (9.0×10^3), 630 (2.2×10^3), 990 (430), and 1190 (430) nm. At 77 K, no EPR signal was detected for either crushed crystals or frozen CH_2Cl_2 solution.

Attempted Preparation of $[Fe(OEP)(H_2O)_2]ClO_4$. The synthetic method for $[Fe(TPP)(H_2O)_2]ClO_4$[6] was followed. In a typical preparation, Fe(OEP)Cl (200 mg) was dissolved in 100 mL of freshly distilled THF (from CaH_2), $AgClO_4$ (0.5 g) was added, and the solution was stirred for 2 h with temperature of ≤40 °C. The solution was filtered, and 1 mL of 70% $HClO_4$ was added. The solution was then allowed to evaporate under air (~3 days), and large well-formed crystals were isolated. An X-ray analysis shows the product to be $[Fe(OEP)(THF)_2]ClO_4$, which has been reported by Ogoshi et al.[8] We present in this paper a brief summary of these results which are of higher precision than reported previously. Recrystallization of $[Fe(OEP)(H_2O)]ClO_4$ or $Fe(OEP)ClO_4$ in undried or water-treated solvents (THF, CH_2Cl_2) did not give the desired crystalline product either; from THF solution,[9] $[Fe(OEP)(THF)_2]ClO_4$ was always obtained, while, in CH_2Cl_2, $[Fe(OEP)(H_2O)]ClO_4$ was isolated as the major product. Data for $[Fe(OEP)(THF)_2]ClO_4$ are as follows. IR (ν_{ClO_4}): 1090, 623 cm^{-1}. UV–vis–near-IR (CH_2Cl_2): λ_{max} (ϵ) 387 (1.13×10^5), 498 (9.2×10^3), 629 (2.0×10^3) 985 (460), and 1220 (460) nm. At 77 K, an EPR signal with $g = 4.26$ was detected for both crystals and CH_2Cl_2 solution.

X-ray Structure Determinations.[10] **$[Fe(OEP)(H_2O)]ClO_4 \cdot 2H_2O$.** Detailed crystallographic data and parameters for data collection are listed in Table 1. Intensity data were collected in θ shells with θ–2θ scanning with all data with $2\theta \leq 45.78°$ collected when a power failure terminated data collection. The data to parameter ratio was 10.5 for this symmetric data set, and no additional data were deemed necessary. Four standard reflections were measured during data collection to check the possible crystal decay and orientation change; no significant fluctuations were noted. Data were reduced with the profile-fitting algorithm of Blessing; no absorption correction was applied. The structure was solved by using the direct methods program MULTAN. After several cycles of least-square refinement, the probable coordinates for the hydrogen atoms of the ligand water molecule and one of the solvent water molecules were located by difference Fourier syntheses. All porphyrin hydrogen atoms were idealized (C–H = 0.95 Å, $B(H) = 1.2B(C)$) and included in the refinement as fixed contributors. Least-squares refinement with anisotropic thermal parameters for all the non-hydrogen atoms and isotropic thermal parameters for the hydrogen atoms of the ligand water and one of the solvent water molecules led to final discrepancy indices[11] of $R = 0.046$ and $R_2 = 0.064$ for the fit of 458 variables to 4817 data with $F_o \geq 3.0\sigma(F_o)$. Positional coordinates and equivalent isotropic thermal parameters are presented in Table 2.

Table 1. Crystallographic Data and Data Collection Parameters

	molecule	
	$[Fe(OEP)(H_2O)]ClO_4 \cdot 2H_2O$	$[Fe(OEP)(THF)_2]ClO_4$
formula	$FeClO_7N_4C_{36}H_{50}$	$FeClO_6N_4C_{44}H_{60}$
fw	742.12	832.29
a, Å	12.169(10)	13.918(8)
b, Å	13.388(11)	16.519(17)
c, Å	13.409(10)	10.654(4)
α, deg	62.71(6)	
β, deg	88.65(6)	118.21(5)
γ, deg	67.97(6)	
V, Å^3	1770.2(2.5)	2158.5(5.3)
space group	$P\bar{1}$	$C2/m$
Z	2	2
d_{calcd}, g/cm^3 (T = 124(1) K)	1.39	1.28
μ, mm^{-1}	0.5521	0.4584
diffractometer	CAD4	FAST
radiation (λ, Å)	Mo Kα (0.710 73)	Mo Kα (0.710 73)
temp, K	124(1)	292(2)
cryst dimens (mm)	0.1 × 0.3 × 0.3	0.15 × 0.25 × 0.33
criterion for observn	$F_o \geq 3.0\sigma(F_o)$	$F_o \geq 2.0\sigma(F_o)$
no. of unique obsd data	4817	2263
R_1	0.046	0.054
R_2	0.064	0.059

$[Fe(OEP)(THF)_2]ClO_4$. A crystal of $[Fe(OEP)(THF)_2]ClO_4$ was mounted on an Enraf-Nonius FAST area-detector diffractometer with a Mo rotating anode source (λ = 0.710 73 Å) operating at 50 kV and 40 mA. The area detector to crystal distance was 40 mm, and the offset angle of the area detector was 25°.[12] The MADNES package was employed for cell constant determination, image measurement, and intensity data evaluation. The X-ray exposure time for each *image* is 10 s, and a total of 1720 images were collected. "Axial photographs" were taken on the FAST to confirm the Laue symmetry, axial lengths, and crystal quality. A total of 4740 measured reflections were considered above background; after averaging, 2271 unique data were available (R_{merge} = 2.5% on F). No absorption correction was deemed necessary. Atomic coordinates of the heavy atoms were taken directly from Ogoshi et al.[8] into least-squares refinement with unit weights. The final value of R_1 was 0.054, and R_2 was 0.059. Positional coordinates for the non-hydrogen atoms are presented in Table 3.

Results

The reaction of the oxo-bridged compound $[Fe(OEP)]_2O$ with aqueous perchloric acid has been found to yield two different crystalline products. These are $\{[Fe(OEP)]_2(OH)\}ClO_4$[5] and $[Fe(OEP)(H_2O)]ClO_4$; the proportions of the two are dependent on the conditions used (cf. Discussion). We have characterized the $[Fe(OEP)(H_2O)]^+$ cation by UV–vis–near-IR, IR, EPR, and Mössbauer spectroscopies, temperature-dependent magnetic susceptibility measurements, and a single-crystal X-ray structure determination. The characterization of $\{[Fe(OEP)]_2(OH)\}ClO_4$ has been previously communicated.[5] We also attempted the synthesis of the diaquo complex $[Fe(OEP)(H_2O)_2]ClO_4$, but these

(8) Masuda, H.; Taga, T.; Osaki, K.; Sugimoto, H.; Yoshida, Z.; Ogoshi, H. *Bull. Chem. Soc. Jpn.* **1982**, *55*, 3891.

(9) Fe(OEP)Cl and $[Fe(OEP)(H_2O)]ClO_4$ are barely soluble in THF. To increase the solubility, 10% CH_2Cl_2 was added. The solution was then stirred with water to make sure it was "wet". Even from this reaction solvent, only $[Fe(OEP)THF)_2]ClO_4$ was obtained.

(10) Programs used in this study include the following. (a) Data reduction for CAD4 data: Blessing, R. H. *Cryst. Rev.* **1987**, *1*, 3. (b) FAST data collection used MADNES routines (J. W. Pflugrath, Cold Spring Harbor, and A. Messerschmidt, Max-Plank-Institute für Biochemie, Martinsried, Germany, unpublished) and data reduction the program ABSURD (I. Tickle, Birbeck College, and P. Evans, MRC, unpublished). (c) Direct method program MULTAN: Main, P.; Hull, S. E.; Lessinger, L.; Germain, G.; Declerq, J.-P.; Woolfson, M. M. MULTAN, a system of computer programs for the automatic solution of crystal structures from X-ray diffraction data. Universities of York, U.K., and Louvain, Belgium. (d) Zalkin's FORDAP for difference Fourier syntheses. (e) Local modified least-square refinement: Lapp, R. L.; Jacobson, R. A. ALLS, a generalized crystallographic least-squares program, National Technical Information Services IS-4708 UC-4, Springfield, VA. (f) Busing and Levy's ORFFE and ORFLS and Johnson's ORTEP2. (g) Atomic form factors: Cromer, D. T.; Mann, J. B. *Acta Crystallogr., Sect. A* **1968**, *24*, 321. Real and imaginary corrections for anomalous dispersion in the form factor of the iron and chlorine atoms: Cromer, D. T.; Liberman, D. J. *J. Chem. Phys.* **1970**, *53*, 1891. Scattering factors for hydrogen: Stewart, R. F.; Davidson, E. R.; Simpson, W. T. *Ibid.* **1965**, *42*, 3175.

(11) $R_1 = \Sigma||F_o| - |F_c||/\Sigma|F_o|$ and $R_2 = [\Sigma w(|F_o| - |F_c|)^2/\Sigma w(F_o)^2]^{1/2}$.

(12) These settings approximately provide a hemisphere of data out to a 2θ angle of 55°.

Table 2. Fractional Coordinates of $[Fe(OEP)(H_2O)]ClO_4 \cdot 2H_2O$[a]

atom	x	y	z
Fe	0.10957(3)	0.33039(3)	0.45013(3)
O(w1)	0.06465(22)	0.21777(21)	0.41170(20)
N(1)	0.24184(21)	0.19428(20)	0.57881(19)
N(2)	0.23036(20)	0.35490(20)	0.34996(18)
N(3)	−0.01538(20)	0.48489(20)	0.32900(19)
N(4)	−0.00190(20)	0.33105(20)	0.56027(19)
C(a1)	0.22960(26)	0.11832(25)	0.68815(23)
C(a2)	0.36264(25)	0.14204(24)	0.57586(23)
C(a3)	0.35317(25)	0.28520(25)	0.37691(23)
C(a4)	0.20929(26)	0.43791(25)	0.23459(23)
C(a5)	−0.00652(25)	0.55081(25)	0.21573(23)
C(a6)	−0.13387(25)	0.54232(24)	0.33504(24)
C(a7)	−0.12239(25)	0.40823(24)	0.53756(23)
C(a8)	0.01792(26)	0.24301(25)	0.67443(23)
C(b1)	0.34259(26)	0.01768(25)	0.75086(23)
C(b2)	0.42624(26)	0.03389(24)	0.68284(23)
C(b3)	0.40898(25)	0.32602(25)	0.27876(24)
C(b4)	0.31958(26)	0.41795(25)	0.19036(24)
C(b5)	−0.12083(25)	0.64783(24)	0.15075(24)
C(b6)	−0.20016(25)	0.64260(24)	0.22513(24)
C(b7)	−0.17738(25)	0.37034(26)	0.63699(24)
C(b8)	−0.08885(26)	0.26885(26)	0.72242(23)
C(m1)	0.41487(25)	0.18646(25)	0.48215(24)
C(m2)	0.09815(25)	0.52689(25)	0.17233(22)
C(m3)	−0.18417(25)	0.50742(25)	0.43234(24)
C(m4)	0.12512(26)	0.14275(25)	0.73105(23)
C(11)	0.36009(26)	−0.08398(25)	0.87028(24)
C(12)	0.3744(3)	−0.05000(28)	0.96123(26)
C(21)	0.55986(27)	−0.03937(26)	0.71014(25)
C(22)	0.62830(28)	0.01987(29)	0.74116(28)
C(31)	0.54220(26)	0.27686(26)	0.28091(24)
C(32)	0.60487(27)	0.32093(28)	0.33857(27)
C(41)	0.33100(26)	0.49136(26)	0.06832(24)
C(42)	0.37678(29)	0.58780(28)	0.05142(25)
C(51)	−0.14545(25)	0.73403(26)	0.02517(24)
C(52)	−0.1583(3)	0.67737(29)	−0.04746(27)
C(61)	−0.33275(27)	0.71631(26)	0.20041(26)
C(62)	−0.4008(3)	0.6494(3)	0.1837(3)
C(71)	−0.30879(27)	0.42679(27)	0.63968(25)
C(72)	−0.37717(29)	0.3688(3)	0.6085(3)
C(81)	−0.09802(28)	0.19471(28)	0.84481(25)
C(82)	−0.1204(3)	0.0834(3)	0.86949(28)
Cl	−0.08291(7)	0.18857(7)	0.20596(6)
O(1)	−0.10443(23)	0.29340(21)	0.22157(21)
O(2)	−0.10196(22)	0.22575(23)	0.08725(18)
O(3)	−0.16441(24)	0.13581(25)	0.25828(21)
O(4)	0.03763(21)	0.10110(22)	0.25829(21)
O(w2)	0.20914(25)	−0.01517(22)	0.51221(26)
O(w3)	−0.12324(24)	0.13878(24)	0.55601(22)
H(w1a)	0.017(3)	0.246(3)	0.349(3)
H(w1b)	0.120(3)	0.142(4)	0.440(3)
H(w2a)	0.186(5)	−0.042(5)	0.576(5)
H(w2b)	0.169(4)	−0.035(4)	0.475(4)

[a] The estimated standard deviations of the least significant digits are given in parentheses.

Table 3. Fractional Coordinates of $[Fe(OEP)(THF)_2]ClO_4$[a]

atom	x	y	z
Fe	0.0000	0.0000	0.0000
N	−0.06192(17)	0.08551(13)	0.07375(23)
C(a1)	−0.05163(20)	0.16820(16)	0.06666(26)
C(a2)	−0.12452(21)	0.07425(17)	0.14139(29)
C(b1)	−0.10636(21)	0.20954(17)	0.13411(28)
C(b2)	−0.15362(21)	0.15149(17)	0.17743(29)
C(m1)	0.0000	0.20610(22)	0.0000
C(m2)	−0.1547(3)	0.0000	0.1696(4)
C(11)	−0.10694(26)	0.29894(18)	0.1536(3)
C(21)	−0.22337(26)	0.16327(20)	0.2481(4)
C(12)	−0.0060(3)	0.32899(23)	0.2818(4)
C(22)	−0.1613(4)	0.1646(4)	0.4058(5)
O(T)	0.15164(23)	0.0000	0.2038(3)
C(1)	0.2504(7)	0.0251(12)	0.2264(10)
C(2)	0.3314(7)	0.0253(8)	0.3771(9)
C(3)	0.2832(8)	−0.0323(8)	0.4357(9)
C(4)	0.1670(8)	−0.0406(9)	0.3253(9)
Cl	0.0104(9)	0.5000	0.0324(8)
O(1)	0.0884(8)	0.5000	0.1696(12)
O(2)	−0.0920(7)	0.5000	0.0570(13)
O(3)	−0.0295(13)	0.5708(4)	−0.020(3)

[a] The estimated standard deviations of the least significant digits are given in parentheses.

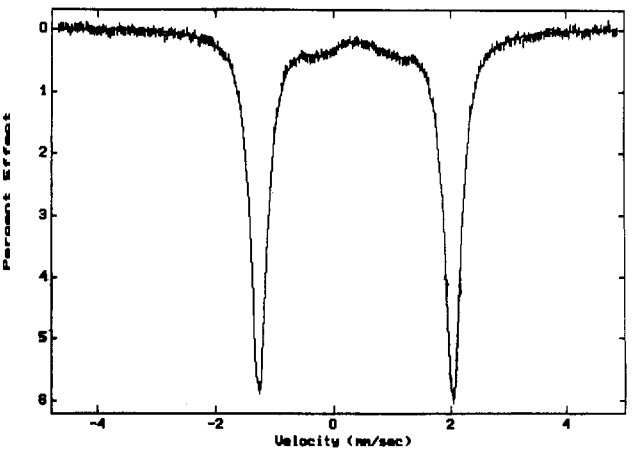

Figure 1. Mössbauer spectrum of $[Fe(OEP)(H_2O)]ClO_4 \cdot 2H_2O$ at 4.2 K and in a field of 2.2 kG perpendicular to the γ beam. The solid line is a Lorentzian fit of the majority species with parameters given in the text and with an 8% admixture of a species with $\Delta E_q = 1.24(4)$ mm/s and an isomer shift of 0.41 mm/s.

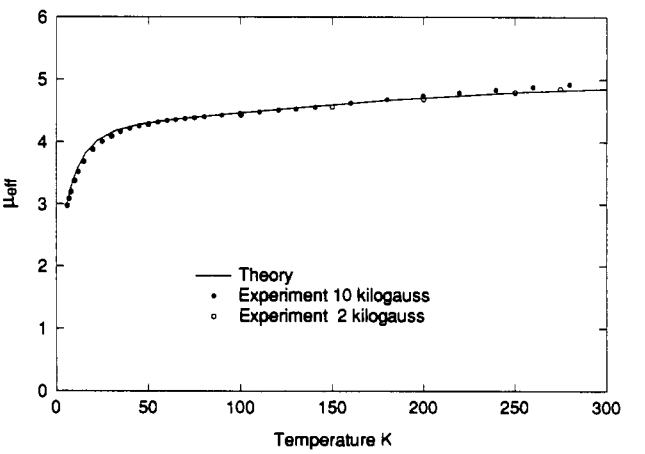

Figure 2. Comparison of observed and calculated values of μ_{eff} vs T for $[Fe(OEP)(H_2O)]ClO_4 \cdot 2H_2O$.

experiments yielded only five-coordinate $[Fe(OEP)(H_2O)]^+$ as a solvated species. Reactions carried out in THF solutions, with varying concentrations of added water, yielded only the previously reported complex $[Fe(OEP)(THF)_2]ClO_4$.[8] The complexes $[Fe(OEP)(H_2O)]ClO_4$, $[Fe(OEP)(OClO_3)]$, and $[Fe(OEP)(THF)_2]ClO_4$ have quite similar electronic spectra, and hence, the probable equilibria among these three species cannot be followed by electronic spectroscopy. Rather, products of the reaction systems were conveniently followed by X-ray identification of the crystalline products.

The low-field Mössbauer spectrum of $[Fe(OEP)(H_2O)]ClO_4$ is shown in Figure 1. The isomer shifts of 0.346(5) mm/s (200 K) and 0.391(5) mm/s (4.2 K) fit the oxidation state of iron(III).[13] The large quadrupole splittings of 3.042(5) mm/s (200 K) and 3.287(5) mm/s (4.2 K) are similar to those observed for a series of five-coordinate, admixed intermediate-spin state iron(III) porphyrinates.[4,14-16] The sample also contains a small amount (≤8%) of a species with $\Delta E_q = 1.24(4)$ mm/s and $\delta =$ 0.41 mm/s. These values are close to those of $\{[Fe(OEP)]_2(OH)\}ClO_4$, and this is the probable impurity.

The temperature-dependent effective magnetic moments of $[Fe(OEP)(H_2O)]ClO_4 \cdot 2H_2O$ are plotted in Figure 2. The general pattern is similar to that observed previously[14] and can be fitted with a modified admixed intermediate-spin Maltempo model.[17]

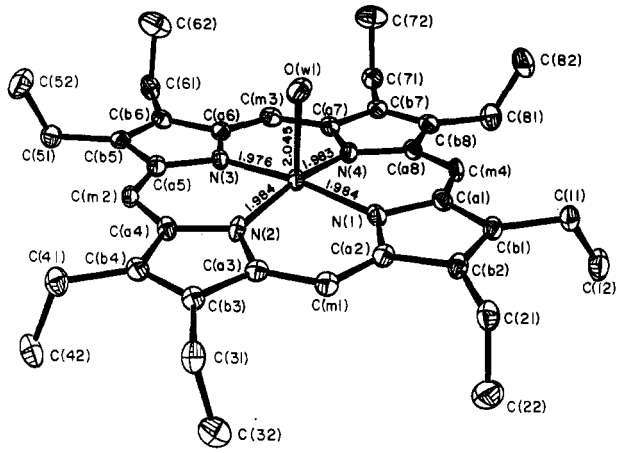

Figure 3. ORTEP drawing of $[Fe(OEP)(H_2O)]ClO_4 \cdot 2H_2O$. Thermal ellipsoids are drawn at the 50% probability level. Porphyrin hydrogen atoms are omitted for clarity.

Table 4. Bond Lengths (Å) in $[Fe(OEP)(H_2O)]ClO_4 \cdot 2H_2O$[a]

Fe–N(1)	1.984(4)	C(b1)–C(b2)	1.362(4)
Fe–N(2)	1.984(3)	C(b3)–C(b4)	1.350(4)
Fe–N(3)	1.976(4)	C(b5)–C(b6)	1.369(4)
Fe–N(4)	1.983(3)	C(b7)–C(b8)	1.361(4)
Fe–O(w1)	2.045(3)	C(b1)–C(11)	1.504(4)
N(1)–C(a1)	1.394(4)	C(b2)–C(21)	1.498(4)
N(1)–C(a2)	1.380(4)	C(b3)–C(31)	1.499(4)
N(2)–C(a3)	1.380(4)	C(b4)–C(41)	1.510(4)
N(2)–C(a4)	1.387(4)	C(b5)–C(51)	1.497(4)
N(3)–C(a5)	1.390(4)	C(b6)–C(61)	1.489(4)
N(3)–C(a6)	1.377(4)	C(b7)–C(71)	1.499(4)
N(4)–C(a7)	1.381(4)	C(b8)–C(81)	1.507(4)
N(4)–C(a8)	1.393(4)	C(11)–C(12)	1.517(4)
C(a1)–C(m4)	1.371(4)	C(21)–C(22)	1.520(4)
C(a2)–C(m1)	1.378(4)	C(31)–C(32)	1.520(4)
C(a3)–C(m1)	1.377(4)	C(41)–C(42)	1.515(4)
C(a4)–C(m2)	1.371(4)	C(51)–C(52)	1.524(4)
C(a5)–C(m2)	1.376(4)	C(61)–C(62)	1.513(5)
C(a6)–C(m3)	1.383(4)	C(71)–C(72)	1.506(4)
C(a7)–C(m3)	1.379(4)	C(81)–C(82)	1.501(5)
C(a8)–C(m4)	1.371(4)	Cl–O(1)	1.440(3)
C(a1)–C(b1)	1.428(4)	Cl–O(2)	1.428(3)
C(a2)–C(b2)	1.435(4)	Cl–O(3)	1.419(3)
C(a3)–C(b3)	1.438(4)	Cl–O(4)	1.422(3)
C(a4)–C(b4)	1.437(4)	O(w1)–H(w1a)	0.87(4)
C(a5)–C(b5)	1.430(4)	O(w1)–H(w1b)	0.88(4)
C(a6)–C(b6)	1.433(4)	O(w2)–H(w2a)	0.85(6)
C(a7)–C(b7)	1.441(4)	O(w2)–H(w2b)	0.89(4)
C(a8)–C(b8)	1.432(4)		

[a] The numbers in parentheses are the estimated standard deviations.

In this model, the two weakly interacting iron(III) centers have parameters $g_\perp = 4.65$, $\zeta = 150$ cm^{-1}, and $J = -1.0$ cm^{-1}.[18] The fit is the solid line in Figure 2. The negative J value is consistent with an antiferromagnetic interaction of the two iron(III) centers, possibly modulated by the π–π interaction between two porphyrin cores within the dimer (Figure 5). The consistency of the magnetic data at 2 and 10 kG indicates an absence of crystal alignment or ferromagnetic impurities.

X-ray Structure of $[Fe(OEP)(H_2O)]ClO_4 \cdot 2H_2O$. The structure of the $[Fe(OEP)(H_2O)]^+$ ion is shown in Figure 3, which also illustrates the labeling scheme for all atoms used in the tables. Individual bond distances and bond angles are given in Tables 4 and 5, respectively. Averaged values for the unique chemical classes of distances and angles in the porphinato core are entered on the mean plane diagram given in Figure 4, which also shows the perpendicular displacements of each atoms (in units of 0.01 Å) from the mean plane of the 24-atom core. The agreement between chemically equivalent bond distances and angles in the core is quite satisfactory. The four Fe–N_p bond distances have an average value of 1.982(4) Å, and the axial Fe–O_{H_2O} bond length is 2.045(3) Å. The displacement of the iron(III) atom

Table 5. Bond Angles (deg) in $[Fe(OEP)(H_2O)]ClO_4 \cdot 2H_2O$[a]

N(1)FeN(2)	89.49(12)	N(4)C(a8)C(m4)	123.71(27)
N(1)FeN(3)	170.03(9)	C(b8)C(a8)C(m4)	125.04(26)
N(1)FeN(4)	89.20(12)	C(a1)C(b1)C(b2)	107.22(25)
N(2)FeN(3)	89.24(12)	C(a1)C(b1)C(11)	124.15(27)
N(2)FeN(4)	166.57(9)	C(b2)C(b1)C(11)	128.63(27)
N(3)FeN(4)	89.74(12)	C(a2)C(b2)C(b1)	106.59(26)
N(1)FeO(w1)	95.13(12)	C(a2)C(b2)C(21)	124.25(27)
N(2)FeO(w1)	99.28(11)	C(b1)C(b2)C(21)	129.11(26)
N(3)FeO(w1)	94.84(12)	C(a3)C(b3)C(b4)	106.74(25)
N(4)FeO(w1)	94.14(11)	C(a3)C(b3)C(31)	124.55(26)
FeN(1)C(a1)	126.67(20)	C(b4)C(b3)C(31)	128.63(26)
FeN(1)C(a2)	127.96(20)	C(a4)C(b4)C(b3)	107.07(25)
C(a1)N(1)C(a2)	104.71(25)	C(a4)C(b4)C(41)	125.35(27)
FeN(2)C(a3)	127.55(19)	C(b3)C(b4)C(41)	127.53(26)
FeN(2)C(a4)	127.74(20)	C(a5)C(b5)C(b6)	106.58(25)
C(a3)N(2)C(a4)	104.44(24)	C(a5)C(b5)C(51)	125.16(26)
FeN(3)C(a5)	127.22(20)	C(b6)C(b5)C(51)	128.24(26)
FeN(3)C(a6)	127.34(20)	C(a6)C(b6)C(b5)	107.01(26)
C(a5)N(3)C(a6)	105.05(24)	C(a6)C(b6)C(61)	124.06(26)
FeN(4)C(a7)	127.73(20)	C(b5)C(b6)C(61)	128.72(27)
FeN(4)C(a8)	127.77(20)	C(a7)C(b7)C(b8)	106.30(25)
C(a7)N(4)C(a8)	103.86(24)	C(a7)C(b7)C(71)	125.45(27)
FeO(w1)H(w1a)	122.(2)	C(b8)C(b7)C(71)	128.02(26)
FeO(w1)H(w1b)	115.(2)	C(a8)C(b8)C(b7)	106.98(25)
N(1)C(a1)C(b1)	110.47(26)	C(a8)C(b8)C(81)	125.16(27)
N(1)C(a1)C(m4)	124.14(27)	C(b7)C(b8)C(81)	127.86(27)
C(b1)C(a1)C(m4)	125.24(27)	C(a2)C(m1)C(a3)	124.86(28)
N(1)C(a2)C(b2)	110.94(26)	C(a4)C(m2)C(a5)	125.26(26)
N(1)C(a2)C(m1)	124.54(27)	C(a6)C(m3)C(a7)	124.49(27)
C(b2)C(a2)C(m1)	124.51(27)	C(a8)C(m4)C(a1)	126.05(26)
N(2)C(a3)C(b3)	110.99(26)	C(b1)C(11)C(12)	113.34(25)
N(2)C(a3)C(m1)	125.18(26)	C(b2)C(21)C(22)	112.62(25)
C(b3)C(a3)C(m1)	123.79(26)	C(b3)C(31)C(32)	111.78(24)
N(2)C(a4)C(b4)	110.69(26)	C(b4)C(41)C(42)	113.08(25)
N(2)C(a4)C(m2)	124.19(26)	C(b5)C(51)C(52)	113.59(25)
C(b4)C(a4)C(m2)	125.12(26)	C(b6)C(61)C(62)	111.12(26)
N(3)C(a5)C(b5)	110.69(26)	C(b7)C(71)C(72)	111.20(25)
N(3)C(a5)C(m2)	124.66(27)	C(b8)C(81)C(82)	114.36(26)
C(b5)C(a5)C(m2)	124.65(27)	O(1)ClO(2)	110.28(17)
N(3)C(a6)C(b6)	110.66(26)	O(1)ClO(3)	108.94(17)
N(3)C(a6)C(m3)	125.36(26)	O(1)ClO(4)	108.56(16)
C(b6)C(a6)C(m3)	123.97(27)	O(2)ClO(3)	108.80(16)
N(4)C(a7)C(b7)	111.59(25)	O(2)ClO(4)	110.41(18)
N(4)C(a7)C(m3)	124.65(26)	O(3)ClO(4)	109.83(18)
C(b7)C(a7)C(m3)	123.74(27)	H(w1a)O(w1)H(w1b)	116.(3)
N(4)C(a8)C(b8)	111.21(26)	H(w2a)O(w2)H(w2b)	99.(4)

[a] The numbers in parentheses are the estimated standard deviations.

from the mean porphinato core is 0.20 Å. The porphinato core also displays a small, but real, S_4-ruffling of the porphyrin core (Figure 4).

Figures 5 and 6 show the interactions between porphyrin molecules in the crystal lattice. In Figure 5, the two "face-to-face" porphyrin rings have a Ct···Ct distance of 4.79 Å, an inter-ring distance of 3.39 Å, and a lateral shift[19] of 3.39 Å. The four "up"/four "down" orientation of the ethyl groups is commonly seen for octaethylporphyrin derivatives with this degree of inter-ring overlap. The dimeric units are extended by the formation of a hydrogen bonding network. As shown in Figure 6, the aquo ligand of one iron in the dimer joins the aquo ligand of an adjacent dimer by hydrogen bonds that also involve solvent water molecules and the perchlorate anions. The hydrogen bond network shown in Figure 6 has an inversion operator located at the center of the network; the six symmetry unique O–H···O distances range from

(13) Debrunner, P. G. *Iron Porphyrins Part 3*; Lever, A. B. P., Gray, H. B., Eds.; VCH: New York, 1989; pp 137–234.
(14) Gupta, G. P.; Lang, G.; Scheidt, W. R.; Geiger, D. K.; Reed, C. A. *J. Chem. Phys.* **1986**, *85*, 5212.
(15) Reed, C. A.; Mashiko, T.; Bentley, S. P.; Kastner, M. E.; Scheidt, W. R.; Spartalian, K.; Lang, G. *J. Am. Chem. Soc.* **1979**, *101*, 2948.
(16) Gupta, G. P.; Lang, G.; Lee, Y. J.; Scheidt, W. R.; Shelly, K.; Reed, C. A. *Inorg. Chem.* **1987**, *26*, 3022.
(17) Maltempo, M. M. *J. Chem. Phys.* **1974**, *61*, 2540.
(18) The Hamiltonian for the evaluation of J has the form $<sc = -JS_1 \cdot S_2$. Complete details of a related analysis are given in ref 14.
(19) Scheidt, W. R.; Lee, Y. J. *Struct. Bonding* **1987**, *64*, 1.

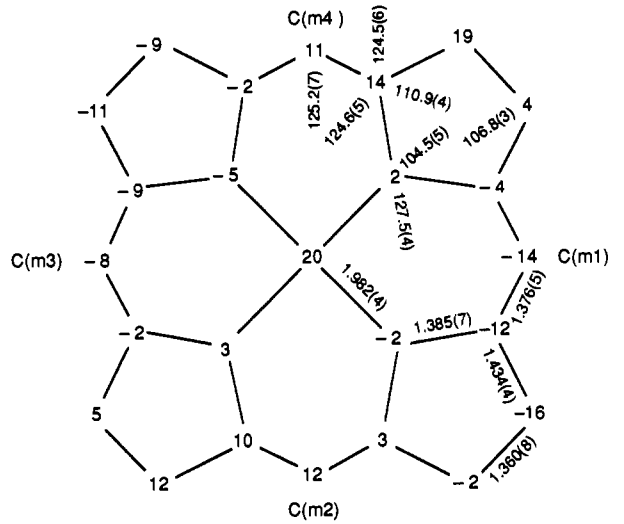

Figure 4. Formal diagram of the porphinato core of $[Fe(OEP)(H_2O)]ClO_4 \cdot 2H_2O$ displaying the average values for the bond parameters. The numbers in parentheses are the estimated standard deviations calculated on the assumption that the averaged values were all drawn from the same population. Also displayed are the perpendicular displacements, in units of 0.01 Å, of each atom from the 24-atom mean plane of the core.

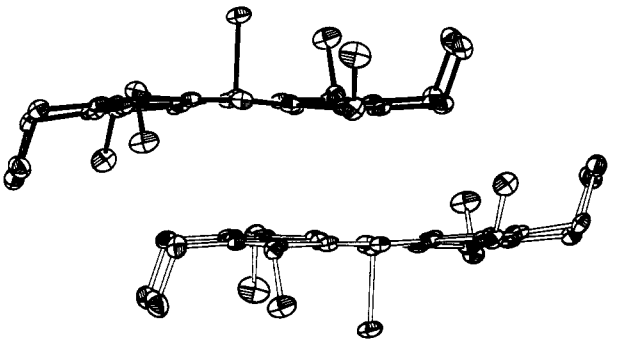

Figure 5. ORTEP drawing showing the close "face-to-face" contact and lateral shift between two $[Fe(OEP)(H_2O)]^+$ ions. Thermal ellipsoids are drawn at the 50% probability level. Porporphyrin hydrogen atoms are omitted for clarity.

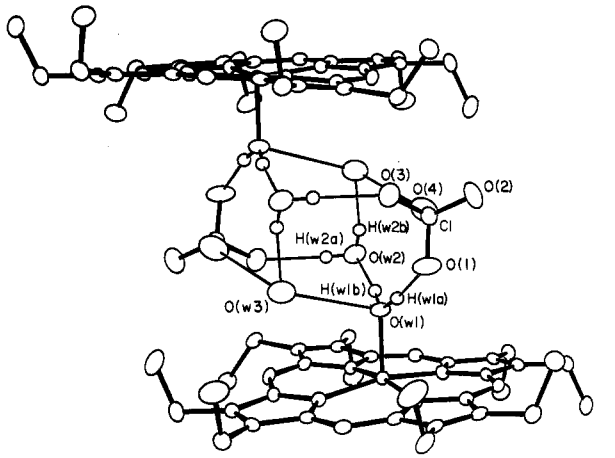

Figure 6. ORTEP drawing showing the hydrogen-bonding network between two molecules of $[Fe(OEP)(H_2O)]ClO_4 \cdot 2H_2O$. A crystallographic inversion center is located at the center of the illustrated hydrogen bond network. Thermal ellipsoids are drawn at the 30% probability level. Porphyrin hydrogen atoms are omitted for clarity.

2.60 to 3.13 Å. There is thus a linear chain of $[Fe(OEP)(H_2O)]^+$ cations in the crystal lattice with alternating π–π and hydrogen bond links.

X-ray Structure of $[Fe(OEP)(THF)_2]ClO_4$. Figure 7 gives the ORTEP diagram for the $[Fe(OEP)(THF)_2]^+$ cation. The cation has both a crystallographically required 2-fold axis and a mirror plane of symmetry, with the iron(III) atom at a symmetry center.

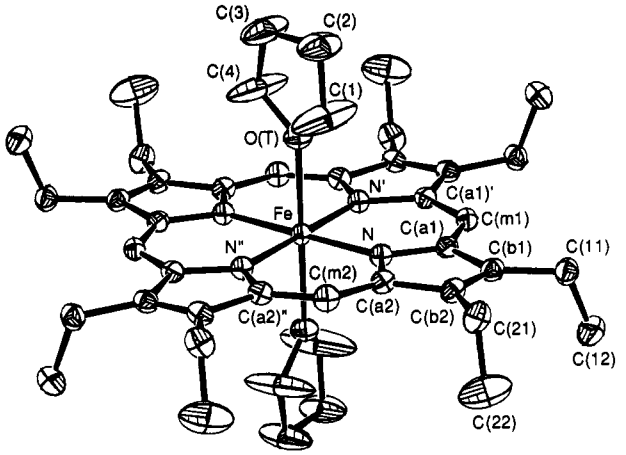

Figure 7. ORTEP drawing of the $[Fe(OEP)(THF)_2]ClO_4$ molecule. Thermal ellipsoids are drawn at the 30% probability level. Porphyrin hydrogen atoms are omitted for clarity.

Table 6. Bond Lengths (Å) and Angles (deg) in $[Fe(OEP)(THF)_2]ClO_4$[a]

Bond Lengths			
Fe–N	1.999(2)	C(11)–C(12)	1.507(5)
Fe–O(T)	2.199(3)	C(21)–C(22)	1.482(6)
N–C(a1)	1.379(4)	O(T)–C(1)	1.344(8)
N–C(a2)	1.381(3)	O(T)–C(4)	1.381(9)
C(a1)–C(b1)	1.442(4)	C(1)–C(2)	1.462(11)
C(a2)–C(b2)	1.444(4)	C(2)–C(3)	1.462(14)
C(a1)–C(m1)	1.377(3)	C(3)–C(4)	1.491(12)
C(a2)–C(m2)	1.375(3)	Cl–O(1)	1.347(12)
C(b1)–C(b2)	1.361(4)	Cl–O(2)	1.565(18)
C(b1)–C(11)	1.492(4)	Cl–O(3)	1.301(11)
C(b2)–C(21)	1.496(4)		

Bond Angles			
N–Fe–N′	90.07(13)	C(a2)–C(b2)–C(21)	125.36(26)
N–Fe–N″	89.93(13)	C(21)–C(b2)–C(b1)	127.71(27)
O(T)–Fe–N	90.15(9)	C(b1)–C(11)–C(12)	112.84(27)
O(T)–Fe–N′	89.85(9)	C(b2)–C(21)–C(22)	113.75(29)
Fe–N–C(a1)	127.09(17)	C(a1)–C(m1)–C(a1)′	125.9(4)
Fe–N–C(a2)	127.27(18)	C(a2)–C(m2)–C(a2)″	126.2(3)
C(a1)–N–C(a2)	105.64(21)	Fe–O(T)–C(1)	126.8(4)
N–C(a1)–C(b1)	110.40(23)	Fe–O(T)–C(4)	125.2(4)
N–C(a1)–C(m1)	124.88(25)	C(1)–O(T)–C(4)	106.8(6)
C(m1)–C(a1)–C(b1)	124.68(26)	O(T)–C(1)–C(2)	112.9(8)
N–C(a2)–C(b2)	110.18(23)	O(T)–C(4)–C(3)	108.9(8)
N–C(a2)–C(m2)	124.59(26)	C(1)–C(2)–C(3)	101.3(8)
C(m2)–C(a2)–C(b2)	125.22(25)	C(2)–C(3)–C(4)	105.6(8)
C(a1)–C(b1)–C(b2)	106.80(24)	O(1)–Cl–O(2)	99.(1)
C(a1)–C(b1)–C(11)	125.23(26)	O(1)–Cl–O(3)	115.(1)
C(11)–C(b1)–C(b2)	127.95(26)	O(2)–Cl–O(3)	80.(1)
C(a2)–C(b2)–C(b1)	106.92(23)	O(3)–Cl–O(3)″	128.(2)

[a] The numbers in parentheses are the estimated standard deviations. The one-primed atom notes the atom translated by a 2-fold axis; the two-primed atom notes the atom translated by a mirror plane.

The 2-fold axis passes through the iron atom and a pair of meso carbons (C(m1), C(m3)); the mirror plane goes through the iron center, a pair of meso carbons (C(m2), C(m4)), and the oxygen atoms of the THF ligands. The perchlorate anion is found to be disordered around a symmetry center with the chlorine and two oxygen atoms (O(1), O(2)) on the mirror plane and another oxygen atom (O(3)) at a general position. This disorder is the same as that described previously,[8] but the precision of the bond distances and angles (Table 6) is significantly increased.

Discussion

The reaction of the oxo-bridged complex $[Fe(OEP)]_2O$ in acidic media has been found to yield different products depending upon the "acidity" of the reaction medium. (An exact definition of acid concentration is difficult because of the biphasic reaction conditions that are used.) When relatively small amounts of acid are used (0.8–2 equiv of H^+/mol of $[Fe(OEP)]_2O$), the

major isolated product is the novel μ-hydroxo dimer complex $\{[Fe(OEP)]_2(OH)\}^+$.[5] At only slightly higher concentrations of acid (2–4 equiv of H^+), the major product is the monoaquo $[Fe(OEP)(H_2O)]^+$ cation, which can be more readily obtained by use of still higher concentrations of acid (cf. method 2 of Experimental Section). It is probable that Dolphin et al.[4] prepared the $[Fe(OEP)(H_2O)]^+$ cation as part of their reported procedure for the preparation of $Fe(OEP)ClO_4 \cdot 2EtOH$ and $Fe(OEP)ClO_4$.

The magnetic properties of the $[Fe(OEP)(H_2O)]^+$ cation are those of the now well-known admixed intermediate-spin iron(III) compounds.[14-16] It is interesting to note that the five-coordinate monoaquo $[Fe(OEP)(H_2O)]^+$ cation has an admixed intermediate-spin state, while the six-coordinate diaquo $[Fe(TPP)(H_2O)_2]^+$ cation has a high-spin state.[23b] This difference follows the earlier suggestion of Scheidt and Reed[20] that a *decrease* in the axial ligand field strength favors the lower of the two spin multiplicities. This is the opposite of that observed in more symmetrical ligand fields and has its origins in the marked tetragonality of iron(III) porphyrinates with weak-field axial ligands. However, the observed spin state of $[Fe(OEP)(H_2O)]^+$ and $[Fe(TPP)(H_2O)_2]^+$ must be influenced by the differences in porphyrin ligands. To delineate the relative importance of these effects, a comparison of the magnetic properties of $[Fe(OEP)(H_2O)]ClO_4$ and $[Fe(OEP)(H_2O)_2]ClO_4$ would be desirable.

We have been unable to prepare the six-coordinate $[Fe(OEP)(H_2O)_2]^+$ complex using the synthetic procedures employed for the $[Fe(TPP)(H_2O)_2]^+$ cation.[6] Surprisingly, tetrahydrofuran coordination to iron(III) in (octaethylporphinato)iron(III) derivatives is favored over water even in THF solvent systems having significantly higher concentrations of water.[9] Crystallization experiments in solvent systems in which water is the only possible ligand yield only the monoaquo $[Fe(OEP)(H_2O)]^+$ cation.[21] The lack of a diaquo species is probably the result of porphyrin π–π interactions which favor dimerization and extrusion of the intervening ligands. An alternative explanation, which we believe less likely, is that the isolation of the $[Fe(OEP)(H_2O)]_2^{2+}$ dimers may simply reflect that the solubility of the π–π dimer is less than any other solution species. EPR measurements were also employed to detect the possible formation of a $[Fe(OEP)(H_2O)_2]^+$ species. At 77 K, isolated $[Fe(OEP)(H_2O)]ClO_4$ has no detectable EPR signal. Discrete $[Fe(OEP)(H_2O)_2]^+$ ions would be expected to have a signal because the TPP analogue does.[6] Since no EPR signals are detected for the "wet" solution systems frozen at 77 K, the possible formation of $[Fe(OEP)(H_2O)_2]^+$ in solution would seem to be largely excluded.

The coordination group geometry of the five-coordinate $[Fe(OEP)(H_2O)]^+$ cation is that expected for an admixed intermediate-spin iron(III) porphyrinate. The average equatorial Fe–N_p bond length of 1.982(4) Å is quite comparable to 1.983(16) Å, the averaged value found for five admixed intermediate-spin derivatives with five-coordination.[15,16,22] The iron(III) ion displacement of 0.20 Å from the mean plane of the 24-atom porphinato core is in the middle of the 0.10–0.30-Å displacements previously reported for five-coordinate admixed intermediate-spin iron(III) porphyrinates.[15,16,22] Finally, the axial Fe–O_{H_2O} bond length of 2.045(3) Å is shorter than all known Fe–O distances to neutral oxygen donors in iron(III) porphyrinates (range 2.069–2.134 Å).[23] These are all high-spin six-coordinate derivatives and thus might be expected to have longer axial distances. It is to be noted that the dimeric π–π interaction (vide infra) might be expected to increase the axial Fe–O distance relative to the discrete ion; in manganese(III) a porphyrin–arene π–π interaction increases the axial Mn–O distance by about 0.04 Å.[24,25]

The intermolecular π–π interaction within a pair of $[Fe(OEP)(H_2O)]^+$ cations (Figure 5) is commonly seen in four- and five-coordinate metallooctaethylporphyrinates. The inter-ring contact parameters (Ct···Ct distance = 4.79 Å, lateral shift = 3.39 Å, porphyrin mean plane separation = 3.39 Å) are characteristic of the "I" or intermediate class as described by Scheidt and Lee[19] and lead to a rather close Fe···Fe separation of 5.08 Å. This accounts for the weak antiferromagnetic coupling ($J = -1.0\ cm^{-1}$) and is similar to that observed previously in several other iron(III) π–π dimers: $[Fe(OEP)(2\text{-}MeHIm)]_2^{2+}$ ($J = -0.8\ cm^{-1}$),[26] $[Fe(OEP)(3\text{-}Cl\text{-}Py)]_2^{2+}$ ($J = -0.6\ cm^{-1}$),[22d] and $[Fe(TPP)(B_{11}\text{-}CH_{12})]_2$ ($J = -3.0\ cm^{-1}$).[16]

Our X-ray structure analysis of $[Fe(OEP)(THF)_2]ClO_4$ produced what we believe to be a more precise structure determination compared to the one previously reported by Ogoshi et al.[8] This is the result, at least in part, of the significantly larger number of reflections that we were able to measure (2263 unique data versus 597). Despite the increased number of data used in the least-squares refinement, our discrepancy indices are significantly lower (by ~2.5%). We find an equatorial Fe–N_p bond distance of 1.999(2) Å, a distance that is fully in accord with the 2.003(8) Å average value reported for five different six-coordinate intermediate-spin derivatives.[27,28] On the other hand, Ogoshi et al. report a bond distance of 1.978(12) Å, a short distance almost at the lower limit of six-coordinate ruffled *low-spin* iron(III) porphyrinates. We also find a slight difference in the axial Fe–O distance: our observed distance is 2.199(3) Å, while the previously reported value was 2.187(11) Å.

The subtlety and variety that can be found in iron(III) porphyrin chemistry is well-illustrated by the present study. It is the complementary application of X-ray, Mössbauer, and magnetic susceptibility techniques to the solid state that best reveals the systematic trends that underlie such diverse magnetostructural behavior.

Acknowledgment. We thank the National Institutes of Health for support of this research under Grants GM-38401 and RR-06709 (W.R.S.), GM-23851 (C.A.R.) and GM-16406 (P.G.D.). R.D.O. thanks Prof. George Lang for providing a computer program to calculate effective magnetic moments for coupled Maltempo admixed intermediate-spin systems.

Supplementary Material Available: Table SI, listing complete crystallographic details for $[Fe(OEP)(H_2O)]ClO_4 \cdot 2H_2O$ and $[Fe(OEP)(THF)_2]ClO_4$, Tables SII and SIII, listing anisotropic thermal parameters and fixed hydrogen atom coordinates for $[Fe(OEP)(H_2O)]ClO_4 \cdot 2H_2O$, and Tables SIV and SV, listing anisotropic thermal parameters and fixed hydrogen atom coordinates for $[Fe(OEP)(THF)_2]ClO_4$ (6 pages). Ordering information is given on any current masthead page.

(20) Scheidt, W. R.; Reed, C. A. *Chem. Rev.* **1981**, *81*, 543.
(21) To date, cell constants have been determined for 10 different single crystals from various different reaction systems. All were the same as that of $[Fe(OEP)(H_2O)]ClO_4$.
(22) (a) Masuda, H.; Taga, T.; Osaki, K.; Sugimoto, H.; Yoshida, Z.-I.; Ogoshi, H. *Inorg. Chem.* **1980**, *19*, 950. (b) Shelly, K.; Bartczak, T.; Scheidt, W. R.; Reed, C. A. *Inorg. Chem.* **1985**, *24*, 4325. (c) Shelly, K.; Reed, C. A.; Lee, Y. J.; Scheidt, W. R. *J. Am. Chem. Soc.* **1986**, *108*, 3117. (d) Scheidt, W. R.; Geiger, D. K.; Lee, Y. J.; Reed, C. A.; Lang, G. *Inorg. Chem.* **1987**, *26*, 1039.
(23) (a) Mashiko, T.; Kastner, M. E.; Spartalian, K.; Scheidt, W. R.; Reed, C. A. *J. Am. Chem. Soc.* **1978**, *100*, 6354–6362. (b) Scheidt, W. R.; Cohen, I. A.; Kastner, M. E. *Biochemistry* **1979**, *18*, 3546–3552. (c) Korber, F. C. F.; Lindsay Smith, J. R.; Prince, S.; Rizkallah, P.; Reynolds, C. D.; Shawcross, D. R. *J. Chem. Soc., Dalton Trans.* **1991**, 3291–3293. (d) Scheidt, W. R.; Geiger, D. K.; Lee, Y. J.; Gans, P.; Marchon, J.-C. *Inorg. Chem.* **1992**, *31*, 2660–2663.
(24) Williamson, M. M.; Hill, C. L. *Inorg. Chem.* **1986**, *25*, 4668.
(25) Williamson, M. M.; Hill, C. L. *Inorg. Chem.* **1987**, *26*, 4155.
(26) Scheidt, W. R.; Geiger, D. K.; Lee, Y. J.; Reed, C. A.; Lang, G. *J. Am. Chem. Soc.* **1985**, *107*, 5693–5699.
(27) (a) Summerville, D. A.; Cohen, I. A.; Hatano, K.; Scheidt, W. R. *Inorg. Chem.* **1978**, *17*, 2906. (b) Scheidt, W. R.; Geiger, D. K.; Hayes, R. G.; Lang, G. *J. Am. Chem. Soc.* **1983**, *105*, 2625. (c) Scheidt, W. R.; Geiger, D. K.; Lee, Y. J.; Reed, C. A.; Lang, G. *Inorg. Chem.* **1987**, *26*, 1039. (d) Scheidt, W. R.; Osvath, S. R.; Lee, Y. J.; Reed, C. A.; Shaevitz, B.; Gupta, G. P. *Inorg. Chem.* **1989**, *28*, 1591. (e) Safo, M. K.; Scheidt, W. R.; Gupta, G. P.; Orosz, R. D.; Reed, C. A. *Inorg. Chim. Acta* **1991**, *184*, 251.
(28) This comparison encompasses only derivatives that have planar or nearly planar porphinato cores.